Phase Diversity with Broadband Illumination

Matthew R. Bolcar and James R. Fienup
The Institute of Optics, University of Rochester, Rochester, NY 14627
bolcar@optics.rochester.edu

Abstract: We explore the limitations of phase diversity when a broadband source is present but is assumed to be monochromatic. A new implementation of phase diversity that accounts for broadband sources is also investigated.

OCIS codes: 100.5070 Phase retrieval; 100.3020 Image reconstruction-restoration ; 110.6770 Telescopes

1. Introduction

Phase diversity is a method of image-based wavefront sensing and image restoration that uses a series of blurred images of an extended object or scene to estimate the optical aberrations in the system and the object being imaged [1,2]. Phase diversity has been applied both to correcting systems with monolithic apertures, and to aligning segmented and multi-aperture systems [1,3]. Further work has been done to utilize the unique architecture of such systems to implement a piston form of phase diversity [4] as well as the conventional focus diversity. All of these treatments assumed a monochromatic model of the object.

In reality it is unlikely that an object of interest will be truly monochromatic. Therefore, narrowband spectral filters must be used to enforce the monochromatic constraint for those models, reducing the amount of light available for imaging. Furthermore, broadband imaging may be part of the science requirement, prohibiting the use of such filters. For example, in Fourier transform imaging spectroscopy (FTIS), it is the spectral content of the image that is directly of interest [5].

In this paper we explore the effects of broadband light on a conventional phase-diversity algorithm using digital simulation. We also present a new version of the phase-diversity algorithm that accounts for broadband light while remaining computationally tractable.

2. Phase Diversity: Background

Typical phase-diversity algorithms use nonlinear optimization techniques to match a model estimate to the collected data. This is usually accomplished by maximizing a likelihood function depending on the dominant noise mechanism of a system. For example, in the Gaussian noise regime, the log-likelihood function is given in the Fourier domain by

$$L(f,\alpha) = -\sum_{k=1}^{K}\sum_{u,v}\left|D_k(u,v) - F(u,v)\,S_k(u,v;\alpha)\right|^2 \tag{1}$$

where f are the unknown object parameters (typically $N\times N$ object pixel values), α are the unknown phase parameters (typically J polynomial coefficients), K is the number of diversity images, (u,v) are the Fourier-domain spatial-frequency coordinates, D is the Fourier transform of the detected images, F is the Fourier transform of the current estimate of the object, and S_k is the system optical transfer function (OTF) for the k^{th} diversity image. Equation (1) is to be maximized with respect to the unknown quantities f and α.

To reduce the search space of the nonlinear optimization procedure, the $N\times N$ object parameters can be removed from the problem. After some work, Eq. (1) becomes the Gonsalves metric [6,2]

$$L_{Gon}(\alpha) = \sum_{u,v\in\chi_1}\frac{\left|\sum_{j=1}^{K} D_j(u,v)\,S_j^*(u,v;\alpha)\right|^2}{\sum_{l=1}^{K}\left|S_l(u,v;\alpha)\right|^2} - \sum_{u,v}\sum_{k=1}^{K}\left|D_k(u,v)\right|^2 . \tag{2}$$

Notice that Eq. (2) depends only on the unknown phase parameters α and therefore the search space of the nonlinear optimization routine is greatly reduced. Analytic derivatives of Eq. (2) are easily calculated to avoid finite-difference derivatives and further reduce the computational burden.

In the presence of a broadband light, Eq. (1) becomes

$$L(f,\alpha) = -\sum_{k=1}^{K}\sum_{u,v}\left|D_k(u,v) - \sum_{\lambda} F_\lambda(u,v) S_{k,\lambda}(u,v;\alpha)\right|^2 \tag{3}$$

where λ indexes the spectral bands of the object. Notice that the unknown object parameters and the unknown phase parameters are coupled by the summation over wavelength. This coupling prevents obtaining a closed form solution of the Gonsalves metric. In this case, a simultaneous optimization over the unknown object parameters and unknown phase parameters must be performed.

An alternative is to consider the approximation

$$F_\lambda(u,v) \approx \Phi_\lambda F(u,v), \tag{4}$$

known as the grey-world approximation, which assumes that every pixel in the object has the same spectrum, defined by the spectral coefficient Φ_λ. Under this approximation, Eq. (3) becomes

$$L(f,\alpha) = -\sum_{k=1}^{K}\sum_{u,v}\left|D_k(u,v) - F(u,v)\sum_{\lambda}\Phi_\lambda S_{k,\lambda}(u,v;\alpha)\right|^2, \tag{5}$$

and the unknown object parameters and unknown phase parameters are decoupled, allowing a Gonsalves-like metric to be computed

$$L_{Gon}(\alpha) = \sum_{u,v\in\chi_1}\frac{\left|\sum_{j=1}^{K} D_j(u,v)\sum_{\lambda}\Phi_\lambda S^*_{j,\lambda}(u,v;\alpha)\right|^2}{\sum_{l=1}^{K}\left|\sum_{\lambda}\Phi_\lambda S_{l,\lambda}(u,v;\alpha)\right|^2} - \sum_{u,v}\sum_{k=1}^{K}\left|D_k(u,v)\right|^2. \tag{6}$$

At first the grey-world approximation may seem naive; however, for regions of images of natural scenery, the grey-world approximation proves to be quite robust over moderately large spectral bandwidths. This approximation may also be true for some astronomical images. Furthermore, using Eq. (6) it is possible to estimate the spectral coefficients Φ_λ and gain information about the spectral content of the object from broadband images of it. Analytic gradients of Eq. (6) with respect to the spectral coefficients are easily calculated to improve computational efficiency.

3. Digital Simulations

A series of digital simulations were performed to evaluate the performance of conventional phase diversity when a broadband object is present but is assumed to be monochromatic, i.e. when Eq. (2) is used as the objective function. The performance results were then compared to the case when the grey-world approximation is made and Eq. (6) is used.

The object used for this study was taken from a set of AVIRIS[7] data which consists of spectroscopic images with a spectral resolution of 10 nm. Four diversity images were simulated for each of 10 different wavefront realizations. Each image had a center wavelength of 1 μm and bandwidths between 0 nm and 400 nm. The average simulated wavefront error was 0.28λ RMS. A multi-aperture configuration consisting of 9 circularly arrayed sub-apertures was used for this study. The effects of photon noise, read noise and quantization error were also included, resulting in an average pixel SNR of 800.

Strehl ratio was used as a metric to compare the performance of the two methods. Given a true wavefront optical path difference (OPD), ϕ_{true}, and the wavefront OPD estimated by the phase-diversity algorithm, ϕ_{est}, we calculate the residual OPD error as $\phi_{res} = \phi_{true} - \phi_{est}$. A broadband incoherent point spread function, $s_{res}(x,y)$, is calculated from the residual OPD error, where (x,y) are the image plane pixel indices. The Strehl ratio quantifying the residual error is then defined as

$$\text{Strehl} = \frac{\max\left(s_{res}(x,y)\right)}{\max\left(s_{per}(x,y)\right)} \tag{7}$$

where $s_{per}(x,y)$ is the broadband incoherent point spread function of a perfect, unaberrated system.

4. Simulation Results

Figure 1 shows the results from the digital simulations. Each point of the curve is an average of the Strehl ratio for 10 different wavefront realizations.

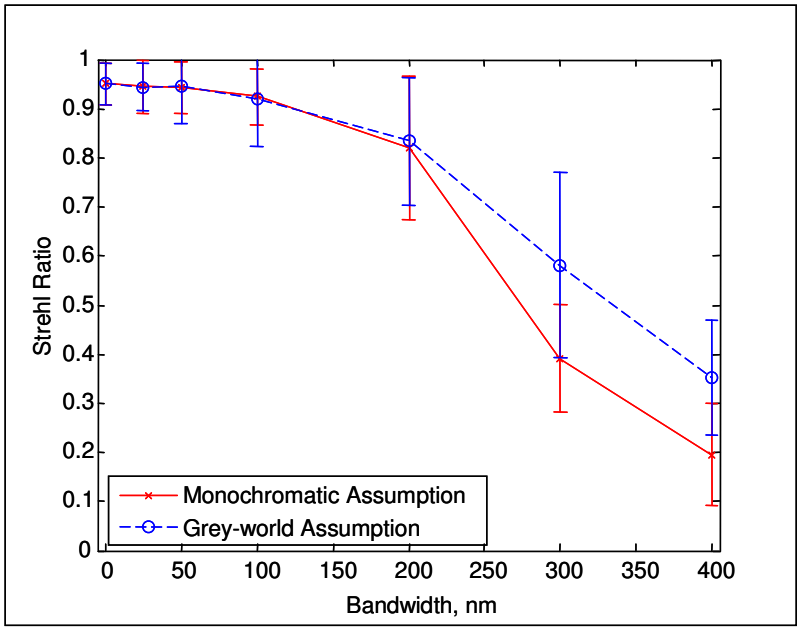

Figure 1 - Digital simulation results. Each point is an average over 10 different wavefront realizations.

For moderately narrow bandwidths between 25 nm and 100 nm, the two methods performed equally well, resulting in Strehl ratios greater than 90%. As the bandwidth increases, however, the grey-world approximation shows an advantage in the estimation error.

5. Conclusions

We have shown that for moderately narrow bandwidths, assuming monochromatic light has little effect on the estimation error of a phase-diversity algorithm. For larger bandwidths, using a grey-world approximation not only results in better estimation of the wavefront, but allows for the estimation of the spectral coefficients as well.

6. Acknowledgements

This research was funded by a NASA Graduate Student Research Program Fellowship, sponsored by Goddard Space Flight Center.

7. References

[1] R.G. Paxman and J.R. Fienup, "Optical misalignment sensing and image reconstruction using phase diversity," *J. Opt. Soc. Am. A* **5**, 914 – 923 (1988).

[2] R.G. Paxman, T.J. Schulz and J.R. Fienup, "Joint estimation of object and aberrations by using phase diversity," *J. Opt. Soc. Am. A* **9**, 1072 – 1085 (1992).

[3] R.L. Kendrick, D.S. Acton and A.L. Duncan, "Phase-diversity wave-front sensor for imaging systems," *Appl. Opt.* **33**, 6533 – 6546 (1994).

[4] M.R. Bolcar and J.R. Fienup, "Method of phase diversity in multi-aperture systems utilizing individual sub-aperture control," in *Unconventional Imaging II*, V.L. Gamiz and P.S. Idell, eds., Proc. SPIE **5896** (2005).

[5] S.T. Thurman and J.R. Fienup, "Multi-aperture Fourier transform imaging spectroscopy: theory and imaging properties," *Opt. Express* **13**, 2160-2175 (2005).

[6] R.A. Gonsalves and R. Chidlaw, "Wavefront sensing by phase retrieval," in *Applications of Digital Image Processing III*, Proc. SPIE **207** (1979).

[7] Provided through the courtesy of Jet Propulsion Laboratory, California Institute of Technology, Pasadena, California (http://aviris.jpl.nasa.gov/).